Bacteria in clouds biodegrade atmospheric formic and acetic acids

Leslie Nuñez López[1], Pierre Amato[1], and Barbara Ervens[1]

[1]Université Clermont Auvergne, CNRS, Institut de Chimie de Clermont-Ferrand, 63000 Clermont-Ferrand, France

Correspondence: Barbara Ervens (barbara.ervens@uca.fr)

Abstract. Formic and acetic acids are major organic species in cloud water and affect precipitation acidity. In current atmospheric models, their losses are limited to chemical oxidation in the gas and aqueous phases and deposition processes. Previous lab studies suggest that these acids can be efficiently biodegraded in water by atmospherically relevant bacteria. However, the importance of biodegradation as a loss process in the atmospheric multiphase system has not been fully assessed. We imple-
5   mented biodegradation as an additional sink of formic and acetic acids in a detailed atmospheric multiphase chemistry model. In our model, biodegradation is considered in a small subset of cloud droplets according to atmospheric bacteria concentrations of $0.1 \, \mathrm{cm}^{-3}$. We predict that up to $20 \, \mathrm{ppt \, h}^{-1}$ formic acid and $5 \, \mathrm{ppt \, h}^{-1}$ acetic acid are biodegraded, affecting the total change of acid concentrations by 20% and 3%, respectively. Our model sensitivity studies suggest that acetic acid is most efficiently biodegraded at high cloud water pH (> 5) whereas biodegradation is least efficient for formic acid under such conditions. This
10   trend is explained by the higher solubility of formic acid (high effective Henry's law constant) that results in less evaporation from bacteria-free and subsequent uptake into bacteria-containing droplets. Our analysis demonstrates that previous estimates of the importance of atmospheric biodegradation were often biased high as they did not correctly account for such diffusion limitation of phase transfer processes between droplets. The results suggest that under specific conditions, biological processes can significantly affect atmospheric composition and concentrations in particular of volatile, moderately soluble organics.

1   Introduction

Small monocarboxylic acids have been of particular interest for several decades as they control to a large extent the acidity of cloud, fog, dew and rain water in regions that are not heavily anthropogenically impacted (Pye et al., 2020). They contribute to up to 60% to the free acidity in remote areas and ~30% in polluted regions (Millet et al., 2015). Recently, it was proposed that the increase in organic particulate matter in continental areas leads to a new chemical regime, in which acid deposition
20   is largely controlled by organic acids, as opposed to previous dominance by secondary inorganic pollutants (sulfate, nitrate) (Lawrence et al., 2023). Formic and acetic acids, the smallest organic acids, are ubiquitous main components of the global organic acid budget (Khare et al., 1999; Paulot et al., 2011). Typical mixing ratios range from 0.015 ppb to 40 ppb for formic and 0.05 ppb to 16 ppb for acetic acid, respectively (Chebbi and Carlier, 1996; Millet et al., 2015). Their direct emission sources include biomass burning, fossil fuel combustion, biogenic sources, and land use activities (Khare et al., 1999; Paulot et al., 2011; Gong et al., 2020). Their abundance in regions far from direct emission sources, e.g., in the Arctic, implies their
formation in the atmosphere (Mungall et al., 2018). Their chemical sources include the oxidation of isoprene-derived products

by ozone or OH in the gas phase (Paulot et al., 2011) and the oxidation of formaldehyde and acetaldehyde by the OH radical in the aqueous phase (Jacob, 1986; Chebbi and Carlier, 1996). Significant fractions ($\sim$20 - 90%) of formic and acetic acids are dissolved in the aqueous phase of clouds comprising a major fraction of the total dissolved organic carbon (Herckes et al.,
30 2013). Therefore, major losses of atmospheric formic and acetic acids include wet deposition and aqueous phase oxidation. Such source and sink processes are included in atmospheric models of various scales (Paulot et al., 2011). The comparison of chemical models to observations shows generally good agreement on a global scale; however, they often reveal discrepancies on regional scales, possibly pointing to inaccurate emission inventories and/or incomplete chemical mechanisms (Franco et al., 2020).

35 Recent lab studies suggest that formic and acetic acids are biodegraded by bacteria under atmospherically relevant conditions (Herlihy et al., 1987; Vaïtilingom et al., 2011; Liu et al., 2023). Bacteria comprise a small number fraction of total atmospheric aerosol particles ($\ll$ 1%) with concentrations on the order of $\sim 10^3$ to 10^5 cells m_{air}^{-3}; this corresponds to 10^3 to 10^5 cells mL_{aq}^{-1} at typical cloud liquid water contents ($\sim$0.1 - 1 g m^{-3}) (Amato et al., 2007). However, to date, biological processes and functions, such as biodegradation, are not included in atmospheric models to describe their potential effects on atmospheric
40 composition, or, in turn, the influence of the atmosphere on the aeromicrobiome (Amato et al., 2023). The consideration of bacteria in models is usually limited to their role as ice nuclei (Fröhlich-Nowoisky et al. (2016) and references therein). However, ice nucleation does not necessarily require living, biologically active cells. The atmosphere is considered a harsh environment for microorganisms due to extreme and rapidly changing conditions in terms of temperature, pH, water and nutrient availability (Amato et al., 2007). Yet, living bacteria cells are commonly found far from emission sources and have
45 been isolated from cloud and fog water, which suggests that clouds may be 'atmospheric oases' for bacteria (Fuzzi et al., 1997; Sattler et al., 2001; Amato et al., 2017; Šantl-Temkiv et al., 2022).

Biodegradation is a well-known efficient aerobic loss process of organics in soil where bacteria cell concentrations are on the order of 10^9 cell cm^{-3} (Adeleke et al., 2017). Species concentrations in the atmosphere are much lower than in the denser soil; however, the atmospheric volume is much larger as compared to the biotic terrestrial and aquatic environments. Therefore,
50 it seems reasonable to infer a potential role of biodegradation as a competitive sink to other atmospheric loss processes. First estimates based on atmospherically relevant cell concentrations and lab-derived biodegradation rates of organic acids suggest that biodegradation might be similarly efficient as OH or NO$_3$ reactions in cloud water (Vaïtilingom et al., 2013; Jaber et al., 2021). However, such processes are not widely included in atmospheric models, mainly due to the lack of comprehensive data sets and appropriate model approaches. Comparing typical number concentrations of cloud droplets ($\sim$50 - 500 cm^{-3}) to those
55 of bacteria cells, it is evident that only a small subset of cloud droplets ($\sim$0.01 - 0.1%) contain a bacteria cell (or possibly a few cells). In the current study, we use a multiphase chemistry model complemented by biodegradation process, to systematically explore the conditions, under which biodegradation of formic and acetic acids by bacteria may be a significant sink in addition to chemical losses. We investigate the sensitivities of the importance of biodegradation to these parameters to wide ranges of cloud droplet diameters and pH values.

2   Description of the multiphase model

2.1   Model equations

We use a multiphase chemistry box model with detailed gas- and aqueous-phase chemistry including 58 reactions in the gas phase and 34 in the aqueous phase (Ervens et al., 2014; Khaled et al., 2021). Fifteen of the 31 chemical species are transferred between the gas and aqueous phases. All parameters for the aqueous phase reactions and phase transfer processes are listed in Tables S1 - S4 (Supporting information). We use the standard equations to describe the multiphase chemistry system:

$$\frac{dC_{aq,g}}{dt} = \underbrace{k_{mt}\, LWC \left(C_g - \frac{C_{aq,g}}{LWC\; K_{H(eff)}\; R\, T} \right)}_{phase\, transfer} + \underbrace{S_{aq} - L_{aq}}_{chemical\, processes} - L_{bact} \tag{1}$$

$$\frac{dC_g}{dt} = \underbrace{-k_{mt}\, LWC \left(C_g - \frac{C_{aq,g}}{LWC\; K_{H(eff)}\; R\, T} \right)}_{phase\, transfer} + \underbrace{S_g - L_g}_{chemical\, processes} \tag{2}$$

whereas LWC is the liquid water content (vol vol^{-1}), $K_{H(eff)}$ is the (effective) Henry's law constant [M atm^{-1}], and R the constant for ideal gases (0.082 L atm (mol K)$^{-1}$). All concentrations are expressed in units related to the gas phase volume, mol g$_{air}^{-1}$. The terms S_{aq}, L_{aq}, S_g, L_g denote the chemical sources and losses in the aqueous (aq) and gas (g) phases. L_{bact} refers to the loss rates of formic and acetic acids by biodegradation that occurs in a subset of droplets. We derived 'rate constants' for biodegradation by converting lab-derived biodegradation rates [mol cell^{-1} s^{-1}] into to k_{bact} [L cell^{-1} s^{-1}] (R33 and R34 in Table S1) (Khaled et al., 2021). We use data measured at a temperature of 17°C for *Pseudomonas* sp., being a representative genus for commonly abundant atmospheric bacteria (Vaïtilingom et al., 2011). k_{bact} is multiplied with the (constant) cell concentration of 2·10^8 cells L^{-1} and the modeled organic acid concentrations to obtain L_{bact} [mol L^{-1} s^{-1}]. The phase transfer of soluble gases is described by means of the kinetic mass transfer coefficient k_{mt} (Schwartz, 1986; Nathanson et al., 1996)

$$k_{mt} = \left(\frac{r_d^2}{3\, D_g} + \frac{r_d}{3\, \alpha} \sqrt{\frac{2\pi\, M_g}{R\, T}} \right)^{-1} \tag{3}$$

whereas r_d is the drop radius [cm], D_g the gas phase diffusion coefficient [cm^2 s^{-1}], α the dimensionless mass accommodation coefficient, and M_g the molecular weight [g mol^{-1}].

2.2   Model initialization and simulations

The box model includes a monodisperse drop population with a constant liquid water content of 0.42 g m^{-3}. Simulations are performed at constant temperature (286 K) and air density (1.032·10^{-3} g cm^{-3}). Drop diameter D_d and number concentration N_d are kept constant throughout each simulation. The model is initialized with the mixing ratios summarized in Table S5. The pH value is fixed throughout each simulation. All simulations are performed for one hour. This period reflects multiple cloud

cycles for a single particle (e.g., bacteria cell) given the lifetime of droplets on the order of ~ 10 - 30 min (Ervens et al., 2008). Simulations are performed for 30 pH values ($3 \leq$ pH ≤ 6) and 30 drop diameters ($1\,\mu m \leq D_d \leq 30\,\mu m$). Given the constant LWC, the total drop number concentration N_d increases with decreasing D_d:

$$N_d \propto \frac{6\,LWC}{\pi\,D_d^3} \tag{4}$$

In the reference set of 900 simulations, no bacteria are considered ($L_{bact} = 0$), i.e. all droplets have the same composition. The results are compared to second set of simulations, in which it is assumed that a small number fraction of the droplets contains bacteria cells ($N_{d2} = N_{cell} = 0.1$ cm$_{\mathrm{air}}^{-3}$). This concentration is at the upper end of atmospheric bacteria cell concentrations. To quantify the importance of biodegradation for each D_d - pH combination, we define the differences between total acid concentrations (gas + aqueous) predicted in the two simulation sets as follows:

$$\Delta C = \mid C_{t,nocell} - C_{t,cell} \mid \tag{5}$$

ΔC represents the absolute difference in predicted total acid concentration (expressed as mixing ratios [ppt]) at the end of the simulation (Figure 1). Thus, it quantifies the extent to which the total acid concentration is overestimated if biodegradation were not included. Accordingly, the relative difference is

$$\Delta C_{rel} = \left| \frac{\Delta C}{C_0 - C_{t,nocell}} \right| \cdot 100\% \tag{6}$$

Depending on model conditions (D_d, pH), the two acids show either a net increase of loss as schematically shown in Figure 1. (All model parameters are defined in Table A1.) Therefore, ΔC_{rel} expresses either the relative extent to which the net increase is reduced or the net loss is enhanced due to biodegradation under the model conditions.
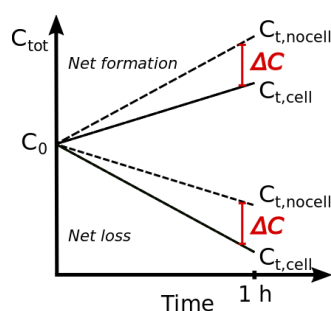
Figure 1. Schematic to illustrate the predicted absolute (ΔC) and relative (ΔC_{rel}) differences in predicted total (gas + aqueous) acid concentrations in the absence ($C_{t,nocell}$) and presence ($C_{t,cell}$) of bacteria cells after one hour simulation time.

3 Model results

3.1 Absolute and relative differences in predicted acid concentrations, ΔC and ΔC_{rel}

Figure 2 shows the predicted absolute concentration difference ΔC from 900 1-hour model simulations as a function of pH value and D_d for formic and acetic acids. The maximum values are $\Delta C_{max} \sim 20$ ppt for formic acid (pH = 4.7, $D_d = 30~\mu$m) and $\Delta C_{max} \sim 8.5$ ppt for acetic acid (pH = 6, $D_d = 27~\mu$m). These values correspond to $\sim 4\%$ of the initial acid mixing ratios of 500 ppt and 200 ppt (Table S5). Both maxima appear at high D_d values but at different pH.

The comparison of the mixing ratios [ppt] of the two acids reveals that they show different trends as a function of pH: Whereas formic acid is predicted to be highest at the highest pH value (Figure S1a,b), the opposite trend is seen for acetic acid (Figure S2a,b). There is a net loss of formic acid at pH $\gtrsim 3.5$ (Figure S1c,d) and net formation of acetic acid (Figure S2c,d), nearly doubling its initial mixing ratio at pH = 6. The resulting relative differences ΔC_{rel} (Equation 6) are shown in panels (e) of Figures S1 and S2. For formic acid, ΔC_{rel} exceeds 100% at pH ~ 3.5; however, these values do not seem meaningful since the absolute change in acid concentration is very small (< 1 ppt). In less acidic droplets, ΔC_{rel} for formic acid decreases from $\sim 50\%$ (pH ~ 4) to < 1% at pH > 5.5. The corresponding values for acetic acid show a continuous increase with increasing pH resulting in $|\Delta C_{rel}| = 2.8\%$ at pH ~ 6 (Figure S2e).

For both acids, biodegradation might lead to decreases in total concentrations on the order of $\sim 4\%$ percent per hour. This corresponds to an enhancement of the formic acid loss rate by up to 20% as compared to chemical losses alone. The net formation rate of acetic acid is reduced by up to 8% under the model conditions. These numbers or trends may increase or decrease in different chemical regimes or may possibly depend on the details of the chemical mechanism; however, the dependence on D_d and pH will be likely robust. In the following, it will be explored why the two acids show differences in the dependency of their biodegradation efficiency on pH and D_d.

3.2 Dependence of ΔC on D_d

Both ΔC and ΔC_{rel} show highest values at largest D_d. To more clearly illustrate this trend, Figure 3a repeats ΔC as a function of D_d along the vertical red lines in Figure 2 at a single pH (pH = 4.6 for formic acid; pH = 5.6 for acetic acid). The drop-size dependence of chemical reactions with organics in the atmospheric multiphase system has been discussed previously. It was demonstrated that organic oxidation tends to be more efficient in small droplets due to higher uptake rates (k_{mt}) in such droplets and resulting enhanced OH(aq) concentrations (Ervens et al., 2014; Chakraborty et al., 2016). Biodegradation apparently shows the opposite trend, i.e. higher efficiency in large droplets (Figure 3a). If OH(aq) were significantly smaller in large droplets, less acid may be oxidized there, leaving higher acid concentrations for biodegradation. However, neither the acid concentrations nor the OH(aq) concentration show any clear trend with drop size (Figure 3b). Therefore, we conclude that diffusion limitation of the reactants into the droplets and competition effects between chemical and biodegradation processes cannot be the main reason for the ΔC dependence on D_d.

A change in D_d leads to a change in the total droplet number concentration N_d, since we assume a constant LWC. The number concentration of bacteria cells ($N_{cell} = 0.1$ cm^{-3}) does not change in our simulations. This implies that the fraction of
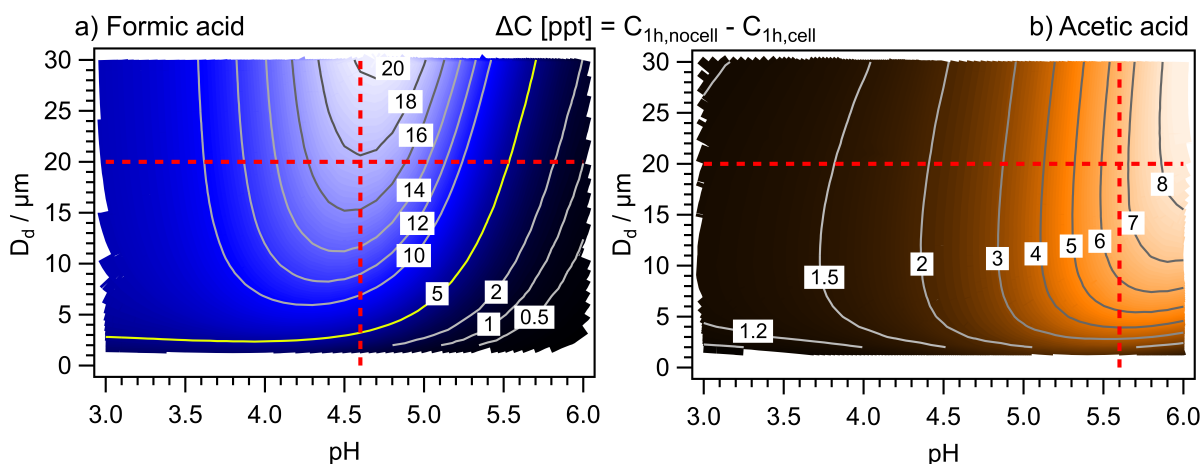
Figure 2. Predicted concentration differences (ΔC; Equation 5) of 900 model simulations for all combinations of 30 pH and 30 D_d values. a) formic acid, b) acetic acid. The red lines denote conditions that are discussed in detail in Section 3.2 and 3.3.

bacteria-containing droplets (F_{NCell}) to total drop number concentration N_d changes with D_d according to

$$F_{NCell} = \frac{N_{cell}}{LWC} \frac{\pi D_d^3}{6} \cdot 100\% \tag{7}$$

Figure 3c shows that F_{NCell} spans several orders of magnitude from $\sim 10^{-4}\%$ to $\sim 0.3\%$. Thus, when droplets are large,

140   biodegradation occurs in a relatively larger fraction of the aqueous phase resulting in relatively more acid being directly accessible for the bacteria. This relationship can explain the trend of an increase in ΔC by a factor of ~ 7 (3 ppt $\leq \Delta C \leq$ 20
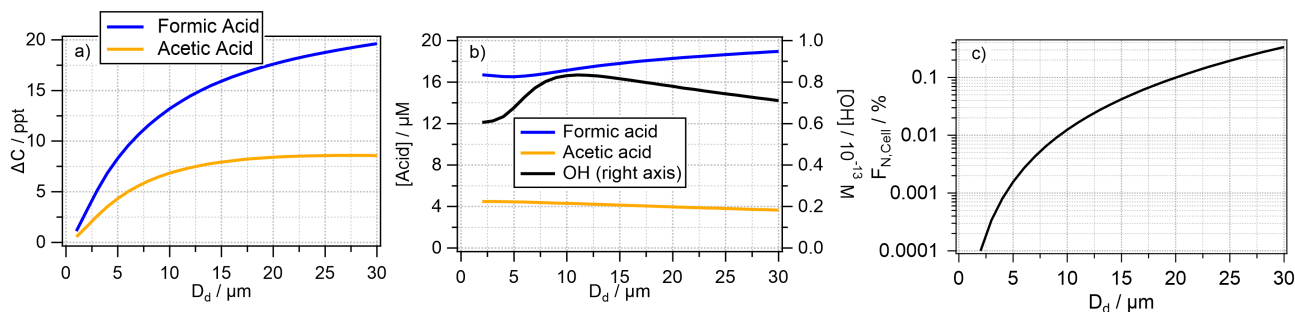
Figure 3. Dependence of a) ΔD of formic acid (pH = 4.6) and acetic acid (pH = 5.6) on the droplet diameter D_d, b) aqueous phase concentrations of formic acid (pH = 4.6) and acetic acid (pH = 5.6) (left scale) and the OH radical (right scale) as a function of D_d, c) the percentage of bacteria-containing droplets F_{NCell} for LWC = 0.42 g m^{-3}, N_{cell} = 0.1 cm^{-3} as a function of D_d.

ppt) for formic acid and by a factor of ~ 3 (2 ppt $\leq \Delta C \leq$ 6 ppt) for acetic acid (Figure 3a). It is not expected that the increase in ΔC is as strong as that for F_{NCell}, since the complex interactions of chemical and phase transfer processes within the

multiphase system do not necessarily translate into linear relationships between loss rates and reaction volume (Section 3.5).

145 A similar increase with D_d as for ΔC is also seen for ΔC_{rel} (Figures S1e and S2e), in particular, for relatively small D_d ($\lesssim$ 10 μm). Based on the ΔC_{rel} values, it may be concluded that a fraction of $\sim$0.01% bacteria-containing cloud droplets may be sufficient to impact the total acid concentrations by several percents. The assumptions of a constant bacteria concentration and varying drop number concentration may represent very specific conditions. Usually, the drop number concentration is a function of the total particle concentration. Under highly polluted conditions often the bacteria concentration scales with the

150 particle number concentration of PM2.5 or PM10 (Gao et al., 2016; Zhai et al., 2018), which may ultimately lead to similar F_{NCell}. Such an increase in N_{cell} may lead to a nearly linear increase in biodegraded mass (Khaled et al., 2021).

3.3 Dependence of ΔC on pH value

Similarly to the analysis in the previous section, Figure 4a shows the ΔC values along the red horizontal lines in Figure 2, i.e. the pH dependence at D_d = 20 μm. Most strikingly, the ΔC trends with pH for the two acids are different with a maximum

155 at pH $\sim$ 4.6 for formic acid and a continuous increase of over the full pH range for acetic acid. ΔC of formic acid spans a range of $\sim$1 to $\sim$17 ppt, while it is smaller for acetic acid with 1 ppt < ΔC < 7 ppt. The biodegradation rates themselves are assumed to be pH-independent, in agreement with lab studies that showed only small variations in biodegradation rates for cloud relevant pH ranges (Liu et al., 2023; Vaïtilingom et al., 2011). The biodegradation rate constants of the two acids differ by less than a factor of two (Table S1) and therefore, it seems unlikely that they cause a significant difference in the

160 general trends of $\Delta C_{(rel)}$ with any parameter. Thus, rather differences in the (physico)chemical properties of the carboxylic acids may be responsible for the trends. Rate constants of OH reactions with undissociated acids k_{RCOOH} are usually smaller than those of the corresponding carboxylates k_{RCOO} due to a shift in the mechanism from H abstraction to electron transfer (Herrmann, 2003). The overall rate constant is a combination of the two rate constants and the proportions of the undissociated acid χ_{RCOOH} and the carboxylate $(1 - \chi_{RCOOH})$ as a function of pH:

165 $$k_{OH,tot} = \chi_{RCOOH} \cdot k_{RCOOH} + (1 - \chi_{RCOOH}) \cdot k_{RCOO} \tag{8}$$

whereas k_{ROO} are the rate constants of R21 and R30 and k_{ROOH} those of R22 and R29 (Table S1), and χ_{RCOOH} is dependent on the acid dissociation constant K_a

$$\chi_{RCOOH} = \left(1 + \frac{K_a}{10^{-pH}}\right)^{-1} \tag{9}$$

$k_{OH,tot}$ is shown for both acids as a function of pH in Figure 4b. The dotted lines in the figure (right axis) illustrate the relative

170 increase normalized to the smallest $k_{OH,tot}$ at pH = 3. This comparison demonstrates that both rate constants increase by a factor of $\sim$5.5 over the pH range between 3 and 6. A high $k_{OH,tot}$ at high pH implies that more acid is chemically degraded at reducing the acid concentration available for biodegradation. This would be opposite to the predicted ΔC trend with pH for acetic acid and could only explain ΔC values above pH $\sim$ 4.6 for formic acid. Thus, the competition of the pH-dependent chemical rate and the biodegradation cannot be the main reason for the apparent pH-dependence of ΔC.
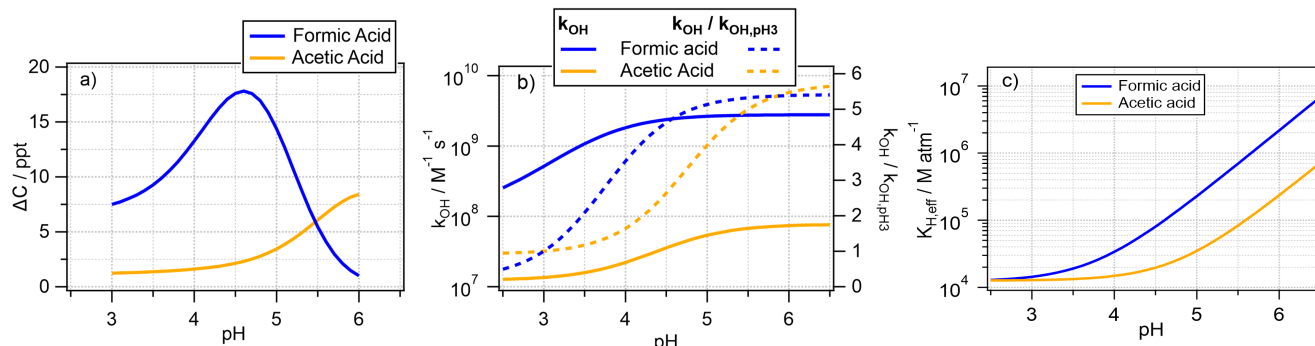
Figure 4. pH dependencies of a) the predicted concentration difference in the absence and presence of bacteria cells (ΔC). b) the total rate constant for the oxidation of formic and acetic acids according to Equation 8; c) effective Henry's law constant

The second pH-dependent parameter that may affect conversion rates in the aqueous phase is the effective Henry's law constant $K_{H,eff}$, the ratio between the total aqueous phase concentration (undissociated acid and carboxylate) and its gas phase partial pressure at thermodynamic equilibrium:

$$K_{H,eff} = \frac{[RCOOH]_{aq} + [RCOO]_{aq}}{[RCOOH]_{gas}} = K_H \cdot \left(1 + \frac{K_a}{[H^+]}\right) \tag{10}$$

K_H is the physical Henry's law constant [M atm^{-1}]. The increase in $K_{H,eff}$ with pH is approximately one order of magnitude higher for formic than for acetic acid (Figure 4c). Therefore, it can be expected that under equilibrium conditions, more formic acid is available for biodegradation leading to a higher ΔC with increasing pH. Given that either pH-dependent parameter $k_{OH,tot}$ and $K_{H,eff}$ can explain some range of the Δ values in subsection 3.3 suggests that a combination of the aqueous phase partitioning and reactivity leads to the differences in the trends shown in Figure 2.

3.4 Dependence of ΔC on the gas-aqueous phase partitioning

The fraction of a compound in the aqueous phase can be defined as

$$\epsilon_{aq} = \frac{C_{aq,g}}{C_{aq,g} + C_g} \tag{11}$$

when aqueous and gas phase concentrations ($C_{aq,g}$ and C_g) are given in identical units, e.g. mol $\text{g}_{\text{air}}^{-1}$. Aqueous phase concentrations C_{aq} as typically given in units of mol $\text{L}_{\text{aq}}^{-1}$ can be converted by

$$C_{aq,g} = 10^{-3} C_{aq} \, LWC \, \rho_{air} \tag{12}$$

At equilibrium conditions (eq), the aqueous phase concentration $C_{aq,g}^{eq}$ is

$$C_{aq,g}^{eq} = K_{H,eff} \, C_g \, LWC \, R \, T \tag{13}$$

The values for ϵ_{aq} at thermodynamic equilibrium (ϵ_{aq}^{eq}) are shown in Figure 5a, overlaid the ΔC values from Figure 4a (dotted lines). It is evident that the decrease in ΔC for formic acid occurs when more than 50% of formic acid is predicted to be in the aqueous phase under equilibrium conditions. The threshold of $\epsilon_{aq}^{eq} = 0.5$ is not reached for acetic acid due to its significantly

195 smaller effective Henry's law constant (smaller K_a, Table S2), and ΔC continues to increase with pH.

The assumption of equilibrium conditions may not be always valid. Species that are very reactive in the aqueous phase are more efficiently consumed than they may be replenished by uptake. To quantify deviations from thermodynamic equilibrium, a parameter q can be used that represents the ratio of the equilibrium concentration to measured or modeled aqueous phase concentrations (Ervens, 2015; Barth et al., 2021):

200
$$q = \frac{C_{aq}}{p_g \, K_{H,eff}} = \frac{\epsilon_{aq}}{1 - \epsilon_{aq}} \frac{1 - \epsilon_{aq}^{eq}}{\epsilon_{aq}^{eq}} \tag{14}$$

whereas p_g corresponds to the gas phase partial pressure [atm]. The resulting values for the bacteria-containing drop class q_{Cell} are shown in Figure 5. It is evident that the acids in the bacteria-containing droplets are in equilibrium at pH = 3 but are increasingly subsaturated at higher pH (Figure 5c). At pH = 5.6, the formic acid concentration is only about 30% of the equilibrium concentration whereas it is nearly 90% for acetic acid. This suggests that at high pH, relatively little formic acid

205 is available for biodegradation resulting in low ΔC values. The higher q_{Cell} value for acetic acid implies that it is closer to equilibrium and, therefore, ΔC values correlate approximately with with $K_{H,eff}$.
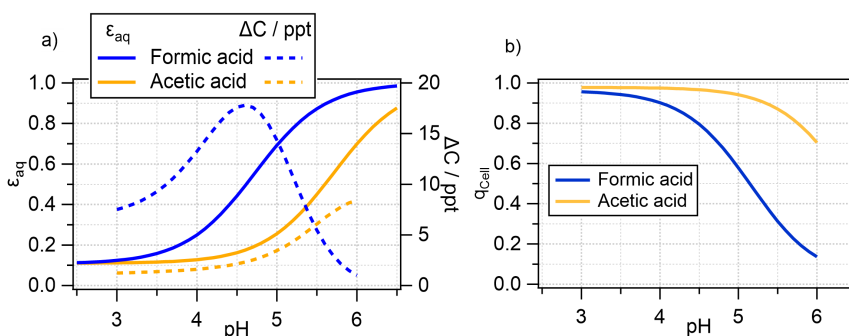
Figure 5. a) Aqueous phase fraction of total formic and acetic acids (undissociated and dissociated) at thermodynamic equilibrium; b) Deviation from thermodynamic equilibrium in the bacteria-containing droplets (D_d = 20 μm; 1-h simulation) (Equation 14); the corresponding q values for bacteria-free droplets are not shown as they are unity, i.e., in thermodynamic equilibrium

These q_{Cell} trends apparently contradict findings from previous measurements or model studies that often have shown that not only formic and acetic acids but also other small organics are in thermodynamic equilibrium in clouds or fog (Winiwarter et al., 1994; Voisin et al., 2000; Facchini et al., 1992; Ervens, 2015). However, it should be kept in mind that the bacteria-

210 containing droplets only comprise 0.1% of all droplets (if D_d = 20 μm, Figure 3c). Such a small deviation would not be detected in measurements of bulk cloud water or in models that focus on the total aqueous phase. In fact, the corresponding predicted q values for the bacteria-free droplets are all unity over the full pH range (not shown).

3.5 Redistribution of acids between the gas phase and droplets

The previous sections point to the competition of the biodegradation with chemical loss processes, but also with the phase

215 transfer to replenish biodegraded acids. To quantify these effects, we compare in the following the individual process rates for

the two acids at different pH values. Figure 6a shows a schematic of all processes considered in the model (Equations 1 and

2). In the bottom panels (b - d) of Figure 6, the relative rates for all processes are shown (at pH values of 3, 4.6, and 5.6),
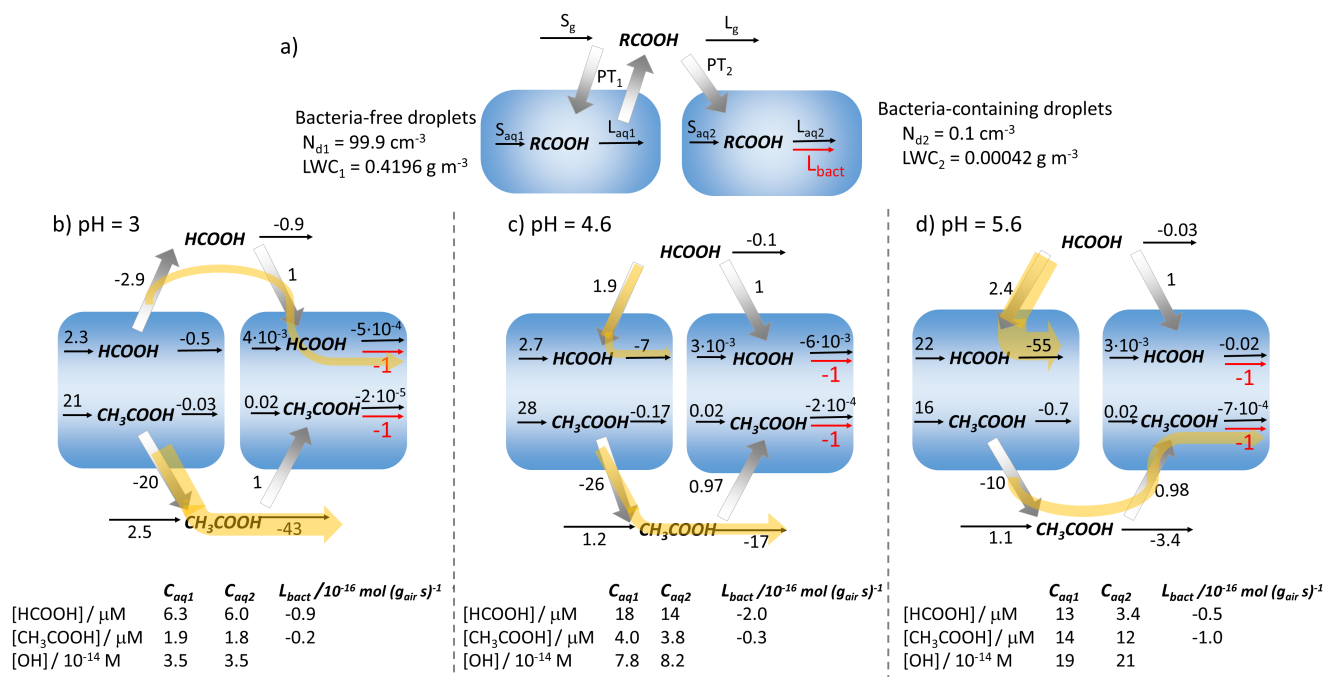
Figure 6. a) Schematic of the chemical sources (S) and losses (L), biodegradation (L_{bact}) and phase transfers (PT) of acids in the gas (g) and aqueous (aq) phases. b) - d) Numbers at the arrows denote the relative rates, normalized to the biodegradation rate L_{bact} [mol g$_{air}^{-1}$ s^{-1}], b) pH = 3; c) pH = 4.6; d) pH = 5.6. Yellow arrows indicate the series of processes that explain the pH dependencies of ΔC and ΔC_{rel} for formic and acetic acids. The tables at the bottom show the aqueous phase concentrations of the acids and the OH radical, together with the absolute value of L_{bact} [10^{-16} mol g$_{air}^{-1}$ s^{-1}]. All results are for 1-hour model simulations, $D_d = 20$ μm

normalized to the biodegradation rate L_{bact} in units of mol g$_{air}^{-1}$s^{-1}. These units are used as they reflect the differences of the

liquid water contents of the two drop classes (999 : 1). Accordingly, the biodegradation rate is indicated as unity. The absolute

220 values for L_{bact} are shown in the last column at the bottom of each panel, together with the aqueous phase concentrations of the

acids and the OH radical. The rates for all processes are summarized in Table S6 (in units of mol g$_{air}^{-1}$ s^{-1} and in mol L$_{aq}^{-1}$ s^{-1}).

At pH = 3, both acids evaporate from the bacteria-free droplets and are taken up by the bacteria-containing droplets. All

chemical loss rates for formic acid are less than unity, i.e. the biodegradation represents the strongest sink in the full multiphase

system, even though it only occurs in 0.1% of the aqueous phase volume. The lack of efficient chemical sinks for formic

explains the high ΔC_{rel} at low pH (Figure S1e). However at this pH, the chemical loss of formic acid is negligible since the oxidation in the gas phase (Rg3, Table S4) is relatively slow, and also the oxidation in the aqueous phase is not efficient due to low $K_{H,eff}$ and $k_{OH,tot}$. The aqueous phase concentrations in the two drop classes do not differ, which suggests that the biodegradation - though *relatively* efficient - does not significantly affect the *absolute* concentration. This explains the small ΔC values at low pH (Figure 2a). This is also reflected in the identical rates within the aqueous phase, if expressed in units of $mol\,L_{aq}^{-1}\,s^{-1}$ (bottom part of Table S6) which would be expected in a system where all droplets are considered identical.

The rate constant of the gas phase loss for acetic acid is an order of magnitude higher than that with formic acid (Rg4, Table S4). This leads to efficient acetic acid loss in the gas phase, exceeding by far (factor 43) the rates of the uptake into the bacteria-containing droplets and and subsequent biodegradation. This results in low values of ΔC_{rel} (Figure S2e). Similarly to formic acid, the chemical rates in the bacteria-containing drop class are not affected by biodegradation, i.e. the total amount of biodegraded acetic acid is very small (low ΔC). The yellow arrows in Figure 6b illustrate the major pathways of the two acids that explain the similarities in ΔC due to the sequence of evaporation, uptake and biodegradation and the differences in terms of loss processes resulting in differences in ΔC_{rel} .

At pH = 4.6, the effective Henry's law constants for formic and acetic acids are higher by factors ~10 and ~2 as compared to pH = 3 (Figure 4c). The increased aqueous phase partitioning leads to higher phase transfer rates into the droplets. Also the rate constants for the aqueous phase loss $k_{OH,tot}$ are higher by factors of 5 and 3 for formic and acetic acids, respectively (Figure 4b). This increased aqueous phase loss leads to a fast consumption and phase transfer of formic acid in all droplets. Most formic acid is taken up by the bacteria-free droplets and consumed there (yellow arrow). However, only about two thirds of formic acid (PT1/PT2 = 1.9/1) are taken up into bacteria-free droplets whereas one third is transferred into the bacteria-containing droplets even though they only comprise 0.1% of the total aqueous phase. The chemical loss rate of formic acid is only seven times higher than the loss by biodegradation (L_{aq1} / L_{bact} = 7) despite the much smaller drop volume. The higher partitioning allows more formic acid to be biodegraded (high ΔC), but its contribution relative to the chemical losses is smaller than at low pH (low ΔC_{rel}). For acetic acid, the increases in $k_{OH,tot}$ and $K_{H,eff}$ are not sufficient to compete with its strong gas phase sink and to shift the direction of the major pathways towards predominating uptake into bacteria-free droplets. Thus, the rate pattern does not change significantly as compared to the lower pH and only results in small increases in both ΔC and ΔC_{rel}.

At pH = 5.6, ~90% of formic acid is expected to partition to the aqueous phase under equilibrium conditions (Figure 5a). However, the concentration in bacteria-containing droplets is only ~30% of this value (Figure 5b). The efficient uptake into the bacteria-free droplets and consumption there dominates the sinks (L_{aq1}/L_{bact} = 55). It leads to even less efficient replenishment of biodegraded acid in the bacteria-containing droplets so that the formic acid concentrations between the droplets classes differ by a factor of ~4 (C_{aq1} = 13 μM, C_{aq2} = 3.4 μM). In a previous model study, even higher concentration differences in bacteria-free and -containing droplets were predicted (Khaled et al., 2021). This led to the conclusion that biodegradation for highly soluble compounds may be inefficient. However, this latter study did not include aqueous phase formation processes (S_{aq}) to provide a continuous acid source (e.g. for formic acid: R7 and R9 in Table S1). With increasing $K_{H,eff}$ and $k_{OH,tot}$ of acetic acid, its gas phase loss becomes relatively less important. Instead the fraction of acetic acid being taken up into the

260 bacteria-containing droplets increases, increasing both ΔC and ΔC_{rel}. Unlike formic acid that is only formed in the aqueous phase, formation of acetic acid also takes place in the gas phase (Rg1, Rg2, Table S4), in addition to its aqueous phase sources (R17 - R19, Table S1). The efficient net production of acetic acid leads to significantly higher total acetic acid concentrations as compared to formic acid, resulting in more acetic acid being degraded at high pH (higher ΔC, Figure 2).

4 Discussion

4.1 Comparison to previous estimates of the importance of biodegradation in the atmosphere: $F_{bact,aq}$ and F_{bact}

The importance of biodegradation has been compared to chemical loss processes in the atmospheric multiphase system in several previous studies. Most of these comparisons limited the comparison to losses in the aqueous phase:

$$F_{bact,aq} = \frac{L_{bact}}{L_{bact} + \underbrace{L_{aq1} + L_{aq2}}_{L_{aq,tot}}} \cdot 100\% \tag{15}$$

Only a few studies extended the comparison to gas phase losses to consider the full atmospheric multiphase system:

270 $$F_{bact} = \frac{L_{bact}}{L_{bact} + \underbrace{L_{aq1} + L_{aq2}}_{L_{aq,tot}} + L_g} \cdot 100\% \tag{16}$$

Table 1 summarizes $F_{bact,aq}$ and F_{bact} values based on literature data for formic and acetic acids and other organics, together with the assumptions made in these comparisons. Most values are based on comparisons of lab-derived biodegradation rates L_{bact} and chemical rates with the OH radical in aqueous solution ('Bulk, $L_{aq,tot}$') (Vaïtilingom et al., 2010, 2011, 2013; Ariya et al., 2002; Liu et al., 2023). Herlihy et al. (1987) reported biodegradation rates of formic and acetic acid observed in

275 incubated rain water. To derive $F_{bact,aq}$, we calculated L_{aq} assuming [OH(aq)] = 10^{-13} M and k_{OH} at pH = 4.6. Similarly, Ariya et al. (2002) compared L_{aq} to biodegradation rates that were estimated after exposing solutions of carboxylic acids to atmospheric fungi in ambient air. Even fewer studies implemented biodegradation into multiphase model studies, applying different assumptions: Pailler et al. (2023) and Jaber et al. (2020) used a multiphase box model with similar LWC and drop sizes as in the current model. They assumed that biodegradation occurs in all droplets, in analogy to chemical reactions. Pailler

280 et al. (2023) used the same lab data for biodegradation rates by Vaïtilingom et al. (2011) as in the current study. However, their model approach implied that the biodegradation rate in each droplet is smaller by a factor $1 / F_{NCell}$ as compared to our approach, where no biodegradation occurs in > 99% of the droplets. In addition, Pailler et al. (2023) describe biodegradation rates as a non-linear function of acid concentrations to account for potential substrate-limitation at low concentrations. In our model study, this relationship is considered being linear for simplicity ($k_{bact} \cdot$[Acid]$_{aq}$). Fankhauser et al. (2019) considered

285 only bacteria-containing droplets, i.e. a total LWC that is several orders of magnitudes smaller than in real clouds ($N_{d1} = 0$). The model approach by Khaled et al. (2021) is similar to the current model. However, they focused on the comparison of loss processes of generic organics over wide ranges of chemical and biodegradation rates and solubility but without any chemical sources.

Table 1. Literature data on the relative importance of biodegradation as compared to chemical processes of organic compounds in the atmospheric aqueous phase $F_{bact,aq}$, (Equation 15) and F_{bact} (Equation 16)

Species	Assumption	pH	$F_{bact,aq}$ / %	F_{bact} / %	Comment	Ref
Monocarboxylic acids						
Formic acid	$L_{aq1} \neq L_{aq2}$ (Fig 6a)	3, 4.6, 5.6	66, 13 , 2	42 , 12 , 2	$\Delta C = 8, 18, 5$ ppt ($D_d = 20\mu$m)	this study
	Bulk $L_{aq,tot}$	5 - 5.3	5.6			[1]
	Bulk $L_{aq,tot}$	$\sim$5, $\sim$6.3	25		pH estimated based on k_{OH}	[2]
	Bulk $L_{aq,tot}$	4, 5, 5	60 , 20, 1		urban; remote; marine	[3]
	Droplets $L_{aq1} = L_{aq2}$	5.5	28	23	Diff in C_{aq} : $\Delta C/C_{nocell}$	[4]
	Incubated rainwater	4.6	12		L_{aq} estimated w [OH]$_{aq}$ = 10^{-13} M	[5]
	$N_{d1}= 0$, $L_{aq1} = 0$	4.5	100	≤ 0.004		[9]
Acetic acid	$L_{aq1} \neq L_{aq2}$ (Fig. 6a)	3, 4.6, 5.6	97 , 87 , 57	2, 6, 19	$\Delta C = 2, 3, 6$ ppt ($D_d = 20\mu$m)	this study
	Bulk $L_{aq,tot}$	5 - 5.3	27			[1]
	Bulk $L_{aq,tot}$	$\sim$5, $\sim$6.3	83		pH estimated based on k_{OH}	[2]
	Droplets $L_{aq1} = L_{aq2}$	5.5	63	7	Diff in C_{aq} : $\Delta C/C_{nocell}$	[4]
	Incubated rainwater	4.6	92		L_{aq} estimated w [OH]$_{aq}$ = 10^{-13} M	[5]
	$N_{d1} = 0$, $L_{aq1} = 0$	4.5	24	≤ 0.004		[9]
Other volatile organics						
Formaldehyde	Droplets $L_{aq1} = L_{aq2}$	5.5	55	5	Diff in C_{aq} : $\Delta C/C_{nocell}$	[4]
	N_{d1}, $L_{aq1} = 0$	4.5	2	≤ 0.004		[9]
Phenol	Bulk $L_{aq,tot}$	4	3	< 0.1	$K_H = 647$ M atm^{-1}	[6]
Catechol	Bulk $L_{aq,tot}$		50	17	$K_H = 8.3 \cdot 10^5$ M atm^{-1}	[6]
Generic organics	$L_{aq1} \neq L_{aq2}$; $S_{g,aq} = 0$		86, 44, 1	6, 40, 1	$K_H = 10^4$; 10^5;10^6	[8]
Non-volatile organics						
Oxalic acid	Bulk $L_{aq,tot}$		0			[2]
	Bulk $L_{aq,tot}$	4, 5, 5	28 , 10 , 1		urban; remote; marine	[3]
	Bulk $L_{aq,tot}$	1.2	98		using [OH$_{aq}$]= 10^{-13} M	[10]
	$N_{d1} = 0$, $L_{aq1} = 0$	4.5	100	≤ 0.004		[9]
Malonic acid	Bulk $L_{aq,tot}$	1.9	43		L_{aq} estimated w [OH]$_{aq}$ = 10^{-13} M	[10]
	$N_{d1} = 0$, $L_{aq1} = 0$	4.5	100	≤ 0.004		[9]
Succinic acid	Bulk $L_{aq,tot}$	5 - 5.3	37			[1]
	Bulk $L_{aq,tot}$	$\sim$5, $\sim$6.3	72			[2]
	Bulk $L_{aq,tot}$	> 4	4		L_{aq} estimated w [OH]$_{aq}$ = 10^{-13} M	[10]
	$N_{d1} = 0$, $L_{aq1} = 0$	4.5	100	≤ 0.004		[9]
Glutaric acid	Bulk $L_{aq,tot}$	> 4	3		L_{aq} estimated w [OH]$_{aq}$ = 10^{-13} M	[10]
Adipic acid	Bulk $L_{aq,tot}$	> 4	3		L_{aq} estimated w [OH]$_{aq}$ = 10^{-13} M	[10]
Pimelic acid	Bulk $L_{aq,tot}$	> 4	1		L_{aq} estimated w [OH]$_{aq}$ = 10^{-13} M	[10]
Amino acids	Bulk $L_{aq,tot}$	6	2 - 99		depending on acid	[7]
Generic organics	$L_{aq1} \neq L_{aq2}$			$\leq F_{cell}$ (Fig. 3c)		[8]

[1] Vaïtilingom et al. (2010); *P. graminis*, [2] Vaïtilingom et al. (2011); [3] Liu et al. (2023); [4] Pailler et al. (2023); summer conditions as [OH]$_{aq}$ most similar to that in Fig. 6d; [5] Herlihy et al. (1987); [6] Jaber et al. (2020); [7] Jaber et al. (2021);[8] Khaled et al. (2021); R_g= 10^{-6} s^{-1}; R_{bact} = 10^{-3} s^{-1}; R_{aq}= 10^{-3} s^{-1}; [9] Fankhauser et al. (2019); [10] Ariya et al. (2002)

Predicted values of $F_{bact,aq}$ for formic acid differ between < 0.004% and 66%. According to our discussion in Section
3.5, the lowest value ($\leq$ 2%) is expected at pH < 5.6. Only the study by Pailler et al. (2023) was performed at such high
pH and resulted in a much higher value (28%). Their bulk model (where biodegradation occurs in all cloud droplets) cannot
represent the redistribution of acids that leads to a reduced L_{bact} at high L_{aq} and $K_{H,eff}$ (Figure 6d). Therefore, their model
overestimates losses by biodegradation for highly soluble species (e.g., formic acid at high pH), as also discussed previously
by (Khaled et al., 2021). Instead of drop classes with significant differences in acid concentration due biodegradation as shown
in Figure 6d, such a bulk model predicts relatively high acid concentrations in all droplets (similar to those as predicted for
bacteria-free droplets in the current simulations). In such a bulk approach, substrate-limited conditions may not be even reached
where biodegradation efficiency becomes negligible below some threshold of substrate (acid) concentration.

Liu et al. (2023) predict decreasing $F_{bact,aq}$ with pH for formic acid. However, the agreement of this trend with our results
in Figure 6 seems fortuitous. In their study, the pH value is considered a proxy for pollution level (urban, remote, marine), and,
thus, not only the pH value but also oxidant levels and bacteria concentrations changed between scenarios. All other values for
$F_{bact,aq}$ in Table 1 that were determined for pH $\leq$ 5 agree approximately with those found in the current study. As discussed
in Section 3.5, under such conditions, the composition of the aqueous phase is not largely affected by biodegradation and
therefore, the assumption of a bulk aqueous phase is applicable for species with chemical reactivity comparable to formic acid.
Similarly, literature values of $F_{bact,aq}$ for acetic acid are in agreement with those found in the current study. Small differences
between the values are expected since different bacteria species and strains were used in the various experiments. The K_H
of phenol is even smaller than that of formic acid and acetic acids at pH = 3. Therefore, its $F_{bact,aq}$ estimated by Jaber et al.
(2020) is likely a good approximation. However, given the much higher K_H of catechol (comparable to $K_{H,eff}$ of formic acid
at pH = 5.6), we conclude that their estimate of $F_{bact(aq)}$ may be too high.

Only a few studies provided values of F_{bact}. The F_{bact} values predicted by Fankhauser et al. (2019) ($\leq$ 0.004%) is orders of
magnitude lower than our results (2 - 42% for formic acid, 2 - 19% for acetic acid). Their value is based on the assumption that
only organics present in bacteria-containing droplets are biodegraded, and they estimate that 0.004% of the atmospheric aque-
ous volume contains bacteria (D_d = 10 μm). However, these considerations neglect the sequence of processes as discussed in
Section 3.5. When acids are chemically formed in bacteria-free-droplets, evaporate and then taken up into bacteria-containing
droplets (Figure 6), contributions by biodegradation can exceed by far the fraction of the aqueous volume where it occurs.
This may ultimately result in biodegradation rates being comparable to chemical loss rates in the total aqueous phase (Ta-
ble S6). Considering bacteria-containing droplets as isolated systems is only appropriate for non-volatile organics, including
(di)carboxylic and amino acids, that are not replenished by phase transfer into bacteria-containing droplets. For such com-
pounds, the upper limit of F_{bact} is indeed constrained by the aqueous phase volume that contains bacteria. This limit may be as
high as 0.3% depending on LWC, N_d and D_d (Figure 3c). For volatile compounds, F_{bact} and $F_{bact,aq}$ values are often similar;
their difference is determined by their reactivity in the gas phase that is relatively low for formic acid, but higher for other
organics, including acetic acid, formaldehyde and phenolic compounds.

4.2 Potential effects of additional microphysical chemical and biological parameters on ΔC, ΔC_{rel}, and F_{bact}

The results discussed in the previous section cover a limited set of cloud microphysical, chemical, and biological parameters. However, based on our sensitivity studies, we can predict trends of the absolute (ΔC) and relative (ΔC_{rel}, F_{bact}) as a function

325 of various parameters as schematically shown in Figure 7.

A monodisperse droplet population is a simplified representation of realistic cloud microphysical properties. The assumption of a polydisperse population with the same LWC and cell concentration distributed randomly across the population will not change F_{NCell} and therefore ΔC is not expected to change. Rates of OH(aq) reactions haven been shown to be enhanced in small droplets and correspondingly decreased in large droplets (Ervens et al., 2014; Chakraborty et al., 2016). These effects

330 might (partially) cancel each other, resulting in a similar total L_{aq} which implies that neither ΔC_{rel} nor F_{bact} will change. An increase in LWC (typically in the range of 0.1 - 1 $\mathrm{g\,m^{-3}}$ for warm clouds) might be caused by a higher droplet number
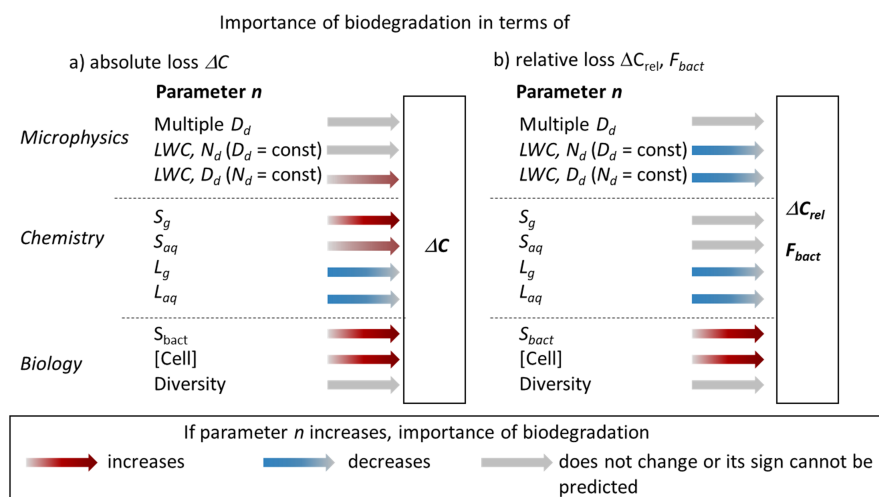
Figure 7. Predicted change of absolute (ΔC) or relative (ΔC_{rel}, F_{bact}) importance of biodegradation as a function of cloud microphysical, chemical, and biological parameters. Red (blue) arrows indicate increased (decreased) importance with an increase of model parameter n; color intensity scales with expected strength of effect. Grey arrows denote either an insignificant change or an unpredictable sign of the change depending on n. These estimates are based on the assumption that one parameter at a time is varied.

concentration (N_d), or larger droplets (D_d) (or a combination of both; Equation 4). An increase in D_d results in an increase in the fraction of bacteria-containing droplets F_{NCell} (Figure 3c), leading to somewhat higher ΔC and ΔC_{rel}. Accordingly, an increase in N_d leads to a decrease in F_{NCell} and to lower ΔC and ΔC_{rel} since the reaction volume for chemical aqueous

335 phase reactions and therefore L_{aq} increase. The absolute amount of acid that is biodegraded ΔC is a function of the number of available cells and, therefore, it is not expected to significantly change as a function of available liquid water. So far, the microphysical parameters LWC, N_d, D_D referred to properties of clouds. Given that also aerosol particles outside clouds

contain liquid water, similar considerations may apply to for such scenarios. Studies of gas-particle partitioning of acids have shown that significant acid fractions are partitioned to particles despite very low LWC ($\sim$10s μg m^{-3}) (Yuan et al., 2015;

340 Nah et al., 2018). If metabolic activity under such water-limited conditions were comparable to that in clouds, ΔC may be comparable if it scales by cell concentration only. There are indications that bacteria are metabolically active outside clouds (Krumins et al., 2014). The relative importance of biodegradation (ΔC_{rel}, $F_{bact(aq)}$) might be even higher than under cloud conditions due to the smaller role of aqueous phase chemical reactions. However, due to the lack of systematic data for biodegradation under such conditions, to date, such comparisons cannot be reliably performed.

345 Chemical models often underpredict observed formic and acetic acid concentrations (Millet et al., 2015). In addition to missing emission sources, recent studies suggested that chemical chemical mechanisms are not complete in terms gas phase sources (Paulot et al., 2011; Yuan et al., 2015; Chen et al., 2021; Gao et al., 2022; Luo et al., 2023). The addition of such formation processes would enhance S_g, leading to higher atmospheric acid concentrations and higher ΔC. However, the higher concentrations would enhance loss rates in both phases so that the ΔC_{rel} might remain constant. In the aqueous phase, the

350 direct oxidation processes of aldehydes (R7 and R19, Table S1) are likely the main sources of formic and acetic acids. However, additional multiphase pathways as suggested by Franco et al. (2021) may occur. Such sources increase S_{aq} in all cloud droplets. Given that most additional acid would be produced in or on bacteria-free droplets, the additional acid directly accessible for the bacteria may be very small leading to a small increase in ΔC. Consequently, ΔC_{rel} may decrease since the increased acid concentration will enhance L_{aq} in the total aqueous volume. Additional acid loss processes of acids in either phase (L_g, L_{aq})

355 lead to a decreased role of biodegradation both in absolute and relative numbers. Such losses may not only include chemical reactions but also acid removal by deposition that is considered a major loss for small acids (Chebbi and Carlier, 1996).

In additional to gaps in chemical mechanisms, current models are even more incomplete with regards to biological processes. Formic and acetic acids may not be only biodegraded but also formed from metabolic processes (Vyas and Gulati, 2009). Such a process could be added as S_{bact} in Figure 6a. Formaldehyde is a likely substrate that may be metabolized and converted into

360 formic acid, in parallel to the chemical pathway R7 (Table S1). The biodegradation rate of formaldehyde is comparable to that of the aqueous phase oxidation (Pailler et al., 2023), S_{bact} could be comparable to L_{bact}. An additional formic acid source in bacteria-containing droplets would enhance ΔC, ΔC_{rel}, and F_{bact}. Depending on the biotransformation efficiency, this process may not only affect the formaldehyde concentration in the bacteria-containing droplets, but possibly even in the full multiphase system. However, due to the lack of data describing such bioformation processes (rates, yields) under atmospherically relevant

365 conditions, they are neglected in our model.

The cell concentration assumed in the current study (0.1 cm^{-3}) is at the upper end of the range of in-cloud observations. Such high concentrations may be particularly relevant in fog close to the ground and/or near strong emission sources of bacteria. All three parameters, ΔC, ΔC_{rel}, and F_{bact} are expected to linearly scale with the concentration of (living, metabolically active) cells Khaled et al. (2021). For simplicity, we assumed that the total bacteria population is composed of metabolically

370 active *Pseudomonas* sp. since they usually represent a major fraction of atmospheric bacteria. However, this assumption underestimates the bacteria diversity in the atmosphere since usually a mixture of different bacteria types and strains are present (Gandolfi et al., 2013). The biodegradation rates of formic and acetic acid span a range of more than an order of magnitude

(Vaïtilingom et al., 2010, 2011). Thus, both the proportions of individual bacteria strains and their different metabolic activities vary depending on the location. It may be speculated that, on average, the consideration of a greater bacteria diversity may not
375   change significantly our results and conclusions for formic and acetic acids. However, more detailed studies are warranted to confirm the validity of this assumption for different locations and atmospheric conditions.

5   Summary and conclusions

Bacteria comprise a ubiquitous, small number fraction of atmospheric aerosol particles. The potential of their metabolic process to affect atmospheric composition has not been widely explored yet. We extended a multiphase box model including detailed
380   gas and aqueous phase chemistry by implementing biodegradation of formic and acetic acids in cloud droplets. Biodegradation is considered in a small subset of the droplets reflecting a typical atmospheric bacteria concentration of 0.1 cm^{-3}. Model studies were performed for a cloud liquid water content (LWC) of 0.42 g m^{-3} with a monodisperse droplet population. To identify scenarios where biodegradation significantly affects formic and acetic acid concentrations, wide ranges of cloud droplet diameters (1 μm $\leq D_d \leq$ 30 μm) and cloud water acidity (3 $\leq$ pH $\leq$ 6) were explored.
385   We predict losses of ΔC $\leq$ 20 ppt h^{-1} and $\leq$ 5 ppt h^{-1} for formic and acetic acids, respectively, corresponding to loss rates of 4% h^{-1} for both acids. This enhances the chemical net loss of formic acid by $\Delta C_{rel} \leq$ 20% and reduces the net formation of acetic acid by $\Delta C_{rel} \leq$ 3% . ΔC and ΔC_{rel} are highest in the presence of large droplets, i.e., when the the total droplet number concentration is small and therefore the fraction of bacteria-containing droplets is largest. The loss by biodegradation increases with pH for acetic acid; however, it reaches its maximum at pH $\sim$ 4.6 for formic acid and decreases at higher pH.
390   The inefficient biodegradation of formic acid at high pH is explained by its strong aqueous-phase partitioning ($K_{H,eff}$ = 8·10^5 M atm^{-1}) and high aqueous phase reactivity (k_{OH} = 3·10^9 M^{-1} s^{-1} at pH = 5.6. These factors lead to the predominant consumption of formic acid in the bacteria-free droplets that comprise > 99% of all cloud droplets. As both the solubility and reactivity of acetic acid are lower at the same pH ($K_{H,eff}$ = 7·10^7 M atm^{-1}, k_{OH} = 8·1^4 M^{-1} s^{-1}), sufficient gas phase acetic acid is available to replenish biodegraded acetic acid in the bacteria-containing droplets.
395   We compared our results to previous estimates of the importance of biodegradation as a loss process in the atmospheric aqueous phase ($F_{bact,aq}$) and in the complete atmospheric multiphase system (F_{bact}). The comparison reveals that the assumption of an averaged biodegradation rate in the full aqueous volume is only appropriate for volatile compounds with low or moderate solubility and aqueous phase reactivity. The role of biodegradation of more highly soluble compounds will be overestimated by a bulk approach, in which biodegradation is assumed to occur in the full aqueous volume, since diffusion-
400   limited phase transfer processes between bacteria-containing and bacteria-free droplets cannot be properly described. For the same reasons, bulk models overestimate the biodegradation of non-volatile species. Due to the separate droplet classes, the upper limit of biodegradable mass of non-volatile species (e.g. dicarboxylic acids) is constrained by the number fraction of bacteria-containing droplets.

We highlight the need of more refined data on the abundance and diversity of (living) bacteria in the atmosphere. Additional
405   biological processes may not only lead to the consumption but also to the formation of organic compounds in clouds, and

possibly also in aqueous aerosol particles outside clouds. We conclude that despite a very small number concentration in the atmosphere ($\leq 0.1\%$ of all aerosol particles and cloud droplets), metabolically active microorganisms (bacteria, fungi, yeast) may be efficient drivers to significantly affect atmospheric concentrations of organic compounds. Our model can be considered a starting point for future studies to further constrain the role of biological processes in the atmosphere to affect biogeochemical

410   cycles in the Earth system.

Table A1. Definition of model parameters

Parameter	Description	Unit
C_{aq}	Aqueous phase concentration	mol $\mathrm{L}_{\mathrm{aq}}^{-1}$
$C_{aq,g}$	Aqueous phase concentration, related to gas volume	mol $\mathrm{g}_{\mathrm{air}}^{-1}$
$C_{aq,g}^{eq}$	Aqueous phase concentration at equilibrium conditions	mol $\mathrm{g}_{\mathrm{air}}^{-1}$
C_g	Gas phase concentration	mol $\mathrm{g}_{\mathrm{air}}^{-1}$
$C_{t,nocell}$	Total acid concentration in the absence of cells	ppt
$C_{t,cell}$	Total acid concentration in the presence of cells	ppt
D_d	Cloud droplet diameter	μm
F_{bact}	Fraction of biodegradation to total (chemical + biological) loss	%
$F_{bact,aq}$	Fraction of biodegradation to total (chemical + biological) loss in the aqueous phase	%
F_{NCell}	Droplet number fraction with bacteria	%
K_H	Physical Henry's law constant	M atm^{-1}
$K_{H,eff}$	Effective Henry's law constant	M atm^{-1}
k_{RCOOH}	Aqueous phase rate constant of OH reactions with undissociated acid	M^{-1} s^{-1}
k_{RCOO}	Aqueous phase rate constant of OH reaction with carboxylate	M^{-1} s^{-1}
$k_{OH,tot}$	pH dependent rate constant of OH reaction with acid and its carboxylate	M^{-1} s^{-1}
L_g	Chemical loss rate in the gas phase	mol $\mathrm{g}_{\mathrm{air}}^{-1}$ s^{-1}
L_{aq}	Chemical loss rate in the aqueous phase	mol $\mathrm{g}_{\mathrm{air}}^{-1}$ s^{-1} or mol $\mathrm{L}_{\mathrm{aq}}^{-1}$ s^{-1}
L_{aq1}	Chemical loss rate in bacteria-free droplets	mol $\mathrm{g}_{\mathrm{air}}^{-1}$ s^{-1} or mol $\mathrm{L}_{\mathrm{aq}}^{-1}$ s^{-1}
L_{aq2}	Chemical loss rate in bacteria-containing droplets	mol $\mathrm{g}_{\mathrm{air}}^{-1}$ s^{-1} or mol $\mathrm{L}_{\mathrm{aq}}^{-1}$ s^{-1}
L_{bact}	Biodegradation rate	mol $\mathrm{g}_{\mathrm{air}}^{-1}$ s^{-1} or mol $\mathrm{L}_{\mathrm{aq}}^{-1}$ s^{-1}
N_d	Total drop number concentration	cm$_{\mathrm{air}}^{-3}$
N_{d1}	Number concentration of bacteria-free droplets	cm$_{\mathrm{air}}^{-3}$
N_{d2}	Number concentration of bacteria-containing droplets	cm$_{\mathrm{air}}^{-3}$
N_{Cell}	Bacterial cell concentration	cm$_{\mathrm{air}}^{-3}$
$PT1$	Phase transfer rate of bacteria-free droplets	mol $\mathrm{g}_{\mathrm{air}}^{-1}$ s^{-1} or mol $\mathrm{L}_{\mathrm{aq}}^{-1}$ s^{-1}
$PT2$	Phase transfer rate of bacteria-containing droplets	mol $\mathrm{g}_{\mathrm{air}}^{-1}$ s^{-1} or mol $\mathrm{L}_{\mathrm{aq}}^{-1}$ s^{-1}
q_{Cell}	Ratio of actual and equilibrium concentrations: $C_{aq,g}$ / $C_{aq,g}^{eq}$	*dimensionless*
S_g	Chemical source rate in the gas phase	mol $\mathrm{g}_{\mathrm{air}}^{-1}$ s^{-1}
S_{aq}	Chemical source rate in the aqueous phase	mol $\mathrm{g}_{\mathrm{air}}^{-1}$ s^{-1} or mol $\mathrm{L}_{\mathrm{aq}}^{-1}$ s^{-1}
S_{aq1}	Chemical source rate in bacteria-free droplets	mol $\mathrm{g}_{\mathrm{air}}^{-1}$ s^{-1} or mol $\mathrm{L}_{\mathrm{aq}}^{-1}$ s^{-1}
S_{aq2}	Chemical source rate in bacteria-containing droplets	mol $\mathrm{g}_{\mathrm{air}}^{-1}$ s^{-1} or mol $\mathrm{L}_{\mathrm{aq}}^{-1}$ s^{-1}
ΔC	Absolute difference in total acid concentration	ppt
ΔC$_{rel}$	Relative difference in total acid concentration	%
ϵ_{aq}	Aqueous phase fraction of total acid	*dimensionless*
ϵ_{aq}^{aq}	Aqueous phase fraction of total acid at thermodynamic equilibrium	*dimensionless*
χ_{RCOOH}	Fraction of undissociated acid	*dimensionless*

Data availability. The dataset related to this work can be accessed via https://doi.org/10.5281/zenodo.8406017

Author contributions. LNL performed the model studies and analysed the results. BE developed the research idea and goals. All authors wrote the manuscript.

Competing interests. One of the authors is a member of the editorial board of Atmospheric Chemistry and Physics.

415 *Acknowledgement.* This work has been supported by the French National Research Agency (ANR), grant no. ANR-17-MPGA-0013.

References

Adeleke, R., Nwangburuka, C., and Oboirien, B.: Origins, roles and fate of organic acids in soils: A review, South African Journal of Botany, 108, 393–406, https://doi.org/10.1016/j.sajb.2016.09.002, 2017.

Amato, P., Parazols, M., Sancelme, M., Laj, P., Mailhot, G., and Delort, A. M.: Microorganisms isolated from the water phase of tropo-
spheric clouds at the Puy de Dôme: Major groups and growth abilities at low temperatures, FEMS Microbiology Ecology, 59, 242–254, https://doi.org/10.1111/j.1574-6941.2006.00199.x, 2007.

Amato, P., Joly, M., Besaury, L., Oudart, A., Taib, N., Moné, A. I., Deguillaume, L., Delort, A. M., and Debroas, D.: Active microorganisms thrive among extremely diverse communities in cloud water, PLoS ONE, 12, 1–22, https://doi.org/10.1371/journal.pone.0182869, 2017.

Amato, P., Mathonat, F., Nuñez Lopez, L., Péguilhan, R., Bourhane, Z., Rossi, F., Vyskocil, J., Joly, M., and Ervens, B.: The
aeromicrobiome: the selective and dynamic outer-layer of the Earth's microbiome., Frontiers in microbiology, 14, 1186 847, https://doi.org/10.3389/fmicb.2023.1186847, 2023.

Ariya, P. A., Nepotchatykh, O., Ignatova, O., and Amyot, M.: Microbiological degradation of atmospheric organic compounds, Geophysical Research Letters, 29, doi:–10.1029/2002GL015 637, 2002.

Barth, M. C., Ervens, B., Herrmann, H., Tilgner, A., McNeill, V. F., Tsui, W. G., Deguillaume, L., Chaumerliac, N., Carlton, A. G., and
Lance, S.: Box Model Intercomparison of Cloud Chemistry, Journal of Geophysical Research Atmospheres, 126, e2021JD035 486, https://doi.org/10.1029/2021JD035486, 2021.

Chakraborty, A., Ervens, B., Gupta, T., and Tripathi, S. N.: Characterization of organic residues of size-resolved fog droplets and their atmospheric implications, Journal of Geophysical Research: Atmospheres, 121, 4317–4332, https://doi.org/10.1002/2015JD024508, 2016.

Chebbi, A. and Carlier, P.: Carboxylic acids in the troposphere, occurrence, sources, and sinks: A review, Atmospheric Environment, 30,
4233–4249, https://doi.org/10.1016/1352-2310(96)00102-1, 1996.

Chen, X., Millet, D. B., Neuman, J. A., Veres, P. R., Ray, E. A., Commane, R., Daube, B. C., McKain, K., Schwarz, J. P., Katich, J. M., Froyd, K. D., Schill, G. P., Kim, M. J., Crounse, J. D., Allen, H. M., Apel, E. C., Hornbrook, R. S., Blake, D. R., Nault, B. A., Campuzano-Jost, P., Jimenez, J. L., and Dibb, J. E.: HCOOH in the remote atmosphere: Constraints from Atmospheric Tomography (ATom) airborne observations., ACS Earth & Space Chemistry, 5, 1436–1454, https://doi.org/10.1021/acsearthspacechem.1c00049, 2021.

Ervens, B.: Modeling the Processing of Aerosol and Trace Gases in Clouds and Fogs, Chemical Reviews, 115, 4157–4198, https://doi.org/10.1021/cr5005887, 2015.

Ervens, B., Carlton, A. G., Turpin, B. J., Altieri, K. E., Kreidenweis, S. M., and Feingold, G.: Secondary organic aerosol yields from cloud-processing of isoprene oxidation products, Geophysical Research Letters, 35, L02 816, https://doi.org/10.1029/2007gl031828, 2008.

Ervens, B., Sorooshian, A., Lim, Y. B., and Turpin, B. J.: Key parameters controlling OH-initiated formation of secondary organic aerosol in
the aqueous phase (aqSOA), J. Geophys. Res. - Atmos., 119, 3997–4016, https://doi.org/10.1002/2013JD021021, 2014.

Facchini, M. C., Fuzzi, S., Lind, J. A., Fierlinger-Oberlinninger, H., Kalina, M., Puxbaum, H., Winiwarter, W., Arends, B. G., Wobrock, W., Jaeschke, W., Berner, A., and Kruisz, C.: Phase-partitioning and chemical rections of low molecular weight organic compounds in fog, Tellus, 44B, 533–544, https://doi.org/10.3402/tellusb.v44i5.15566, 1992.

Fankhauser, A. M., Antonio, D. D., Krell, A., Alston, S. J., Banta, S., and McNeill, V. F.: Constraining the Impact of Bac-
teria on the Aqueous Atmospheric Chemistry of Small Organic Compounds, ACS Earth and Space Chemistry, 3, 1485–1491, https://doi.org/10.1021/acsearthspacechem.9b00054, 2019.

Franco, B., Clarisse, L., Stavrakou, T., Müller, J.-F., Taraborrelli, D., Hadji-Lazaro, J., Hannigan, J. W., Hase, F., Hurtmans, D., Jones, N., Lutsch, E., Mahieu, E., Ortega, I., Schneider, M., Strong, K., Vigouroux, C., Clerbaux, C., and Coheur, P.-F.: Spaceborne Measurements of Formic and Acetic Acids: A Global View of the Regional Sources, Geophysical Research Letters, 47, e2019GL086 239, https://doi.org/10.1029/2019GL086239, 2020.

Franco, B., Blumenstock, T., Cho, C., Clarisse, L., Clerbaux, C., Coheur, P.-F., De Mazière, M., De Smedt, I., Dorn, H.-P., Emmerichs, T., Fuchs, H., Gkatzelis, G., Griffith, D. W. T., Gromov, S., Hannigan, J. W., Hase, F., Hohaus, T., Jones, N., Kerkweg, A., Kiendler-Scharr, A., Lutsch, E., Mahieu, E., Novelli, A., Ortega, I., Paton-Walsh, C., Pommier, M., Pozzer, A., Reimer, D., Rosanka, S., Sander, R., Schneider, M., Strong, K., Tillmann, R., Van Roozendael, M., Vereecken, L., Vigouroux, C., Wahner, A., and Taraborrelli, D.: Ubiquitous atmospheric production of organic acids mediated by cloud droplets, Nature, 593, 233–237, https://doi.org/10.1038/s41586-021-03462-x, 2021.

Fröhlich-Nowoisky, J., Kampf, C. J., Weber, B., Huffman, J. A., Pöhlker, C., Andreae, M. O., Lang-Yona, N., Burrows, S. M., Gunthe, S. S., Elbert, W., Su, H., Hoor, P., Thines, E., Hoffmann, T., Després, V. R., and Pöschl, U.: Bioaerosols in the Earth system: Climate, health, and ecosystem interactions, Atmospheric Research, 182, 346–376, https://doi.org/10.1016/j.atmosres.2016.07.018, 2016.

Fuzzi, S., Mandrioli, P., and Perfetto, A.: Fog droplets - An atmospheric source of secondary biological aerosol particles, Atmospheric Environment, 31, 287–290, https://doi.org/10.1016/1352-2310(96)00160-4, 1997.

Gandolfi, I., Bertolini, V., Ambrosini, R., Bestetti, G., and Franzetti, A.: Unravelling the bacterial diversity in the atmosphere, Applied Microbiology and Biotechnology, 97, 4727–4736, https://doi.org/10.1007/s00253-013-4901-2, 2013.

Gao, M., Yan, X., Qiu, T., Han, M., and Wang, X.: Variation of correlations between factors and culturable airborne bacteria and fungi, Atmospheric Environment, 128, 10–19, https://doi.org/10.1016/j.atmosenv.2015.12.008, 2016.

Gao, Z., Vasilakos, P., Nah, T., Takeuchi, M., Chen, H., Tanner, D. J., Ng, N. L., Kaiser, J., Huey, L. G., Weber, R. J., and Russell, A. G.: Emissions, chemistry or bidirectional surface transfer? Gas phase formic acid dynamics in the atmosphere, Atmospheric Environment, 274, 118 995, https://doi.org/10.1016/j.atmosenv.2022.118995, 2022.

Gong, J., Qi, J., E, B., Yin, Y., and Gao, D.: Concentration, viability and size distribution of bacteria in atmospheric bioaerosols under different types of pollution, Environmental Pollution, 257, 1–11, https://doi.org/10.1016/j.envpol.2019.113485, 2020.

Herckes, P., Valsaraj, K. T., and Collett Jr, J. L.: A review of observations of organic matter in fogs and clouds: Origin, processing and fate, Atmospheric Research, 132–133, 434–449, https://doi.org/10.1016/j.atmosres.2013.06.005, 2013.

Herlihy, L. J., Galloway, J. N., and Mills, A. L.: Bacterial utilization of formic and acetic acid in rainwater, Atmospheric Environment (1967), 21, 2397–2402, https://doi.org/10.1016/0004-6981(87)90374-X, 1987.

Herrmann, H.: Kinetics of aqueous phase reactions relevant for atmospheric chemistry, Chemical Reviews, 103, 4691–4716, 2003.

Jaber, S., Lallement, A., Sancelme, M., Leremboure, M., Mailhot, G., Ervens, B., and Delort, A. M.: Biodegradation of phenol and catechol in cloud water: Comparison to chemical oxidation in the atmospheric multiphase system, Atmospheric Chemistry and Physics, 20, 4987–4997, https://doi.org/10.5194/acp-20-4987-2020, 2020.

Jaber, S., Joly, M., Brissy, M., Leremboure, M., Khaled, A., Ervens, B., and Delort, A. M.: Biotic and abiotic transformation of amino acids in cloud water: Experimental studies and atmospheric implications, Biogeosciences, 18, 1067–1080, https://doi.org/10.5194/bg-18-1067-2021, 2021.

Jacob, D. J.: Chemistry of OH in Remote Clouds and its Role in the Production of Formic Acid and Peroxymonosulfate, Journal of geophysical Research - Atmosphere, 91, 9807–9826, 1986.

Khaled, A., Zhang, M., Amato, P., Delort, A.-M., and Ervens, B.: Biodegradation by bacteria in clouds: an underestimated sink for some organics in the atmospheric multiphase system, Atmospheric Chemistry and Physics, 21, 3123–3141, https://doi.org/10.5194/acp-21-3123-2021, 2021.

Khare, P., Kumar, N., Kumari, K. M., and Srivastava, S. S.: Atmospheric Formic and Acetic Acids: An Overview, Reviews of Geophysics, 37, 227–248, 1999.

Krumins, V., Mainelis, G., Kerkhof, L. J., and Fennell, D. E.: Substrate-Dependent rRNA Production in an Airborne Bacterium, Environmental Science & Technology Letters, 1, 376–381, https://doi.org/10.1021/ez500245y, 2014.

Lawrence, C. E., Casson, P., Brandt, R., Schwab, J. J., Dukett, J. E., Snyder, P., Yerger, E., Kelting, D., VandenBoer, T. C., and Lance, S.: Long-term monitoring of cloud water chemistry at Whiteface Mountain: the emergence of a new chemical regime, Atmospheric Chemistry and Physics, 23, 1619–1639, https://doi.org/10.5194/acp-23-1619-2023, 2023.

Liu, Y., Lim, C. K., Shen, Z., Lee, P. K. H., and Nah, T.: Effects of pH and light exposure on the survival of bacteria and their ability to biodegrade organic compounds in clouds: implications for microbial activity in acidic cloud water, Atmospheric Chemistry and Physics, 23, 1731–1747, https://doi.org/10.5194/acp-23-1731-2023, 2023.

Luo, P.-L., Chen, I.-Y., Khan, M. A. H., and Shallcross, D. E.: Direct gas-phase formation of formic acid through reaction of Criegee intermediates with formaldehyde, Communications Chemistry, 6, 130, https://doi.org/10.1038/s42004-023-00933-2, 2023.

Millet, D. B., Baasandorj, M., Farmer, D. K., Thornton, J. A., Baumann, K., Brophy, P., Chaliyakunnel, S., de Gouw, J. A., Graus, M., Hu, L., Koss, A., Lee, B. H., Lopez-Hilfiker, F. D., Neuman, J. A., Paulot, F., Peischl, J., Pollack, I. B., Ryerson, T. B., Warneke, C., Williams, B. J., and Xu, J.: A large and ubiquitous source of atmospheric formic acid, Atmospheric Chemistry and Physics, 15, 6283–6304, https://doi.org/10.5194/acp-15-6283-2015, 2015.

Mungall, E. L., Abbatt, J. P. D., Wentzell, J. J. B., Wentworth, G. R., Murphy, J. G., Kunkel, D., Gute, E., Tarasick, D. W., Sharma, S., Cox, C. J., Uttal, T., and Liggio, J.: High gas-phase mixing ratios of formic and acetic acid in the High Arctic, Atmospheric Chemistry and Physics, 18, 10 237–10 254, https://doi.org/10.5194/acp-18-10237-2018, 2018.

Nah, T., Guo, H., Sullivan, A. P., Chen, Y., Tanner, D. J., Nenes, A., Russell, A., Ng, N. L., Huey, L. G., and Weber, R. J.: Characterization of aerosol composition, aerosol acidity, and organic acid partitioning at an agriculturally intensive rural southeastern US site, Atmospheric Chemistry and Physics, 18, 11 471–11 491, https://doi.org/10.5194/acp-18-11471-2018, 2018.

Nathanson, G. M., Davidovits, P., Worsnop, D. R., and Kolb, C. E.: Dynamics and Kinetics at the Gas-Liquid Interface, J. Phys. Chem., 100, 13 007–13 020, https://doi.org/10.1021/jp953548e, 1996.

Pailler, L., Wirgot, N., Joly, M., Renard, P., Mouchel-Vallon, C., Bianco, A., Leriche, M., Sancelme, M., Job, A., Patryl, L., Armand, P., Delort, A.-M., Chaumerliac, N., and Deguillaume, L.: Assessing the efficiency of water-soluble organic compound biodegradation in clouds under various environmental conditions, Environmental Science: Atmospheres, 3, 731–748, https://doi.org/10.1039/D2EA00153E, 2023.

Paulot, F., Wunch, D., Crounse, J. D., Toon, G. C., Millet, D. B., Decarlo, P. F., Vigouroux, C., Deutscher, N. M., Abad, G. G., Notholt, J., Warneke, T., Hannigan, J. W., Warneke, C., Gouw, J. A. D., Dunlea, E. J., Mazière, M. D., Griffith, D. W., Bernath, P., Jimenez, J. L., and Wennberg, P. O.: Importance of secondary sources in the atmospheric budgets of formic and acetic acids, Atmospheric Chemistry and Physics, 11, 1989–2013, https://doi.org/10.5194/acp-11-1989-2011, 2011.

Pye, H. O., Nenes, A., Alexander, B., Ault, A. P., Barth, M. C., Clegg, S. L., Collett, J. L., Fahey, K. M., Hennigan, C. J., Herrmann, H., Kanakidou, M., Kelly, J. T., Ku, I. T., McNeill, V. F., Riemer, N., Schaefer, T., Shi, G., Tilgner, A., Walker, J. T., Wang, T., Weber, R., Xing,

J., Zaveri, R. A., and Zuend, A.: The acidity of atmospheric particles and clouds, Atmospheric Chemistry and Physics, 20, 4809–4888, https://doi.org/10.5194/acp-20-4809-2020, 2020.

Šantl-Temkiv, T., Amato, P., Casamayor, E. O., Lee, P. K. H., and Pointing, S. B.: Microbial ecology of the atmosphere, FEMS Microbiology Reviews, p. fuac009, https://doi.org/10.1093/femsre/fuac009, 2022.

530 Sattler, B., Puxbaum, H., and Psenner, R.: Bacterial growth in supercooled cloud droplets, Geophysical Research Letters, 28, 239–242, https://doi.org/10.1029/2000GL011684, 2001.

Schwartz, S.: Mass transport considerations pertinent to aqueous phase reactions of gases in liquid water clouds, in: Chemistry of Multiphase Atmospheric Systems, edited by Jaeschke, W., vol. 6 of *NATO ASI Series*, pp. 415–471, Springer, Berlin, 1986.

Vaïtilingom, M., Amato, P., Sancelme, M., Laj, P., Leriche, M., and Delort, A.-M.: Contribution of Microbial Activity to Carbon Chemistry
535 in Clouds, Applied and Environmental Microbiology, 76, 23–29, https://doi.org/10.1128/AEM.01127-09, 2010.

Vaïtilingom, M., Charbouillot, T., Deguillaume, L., Maisonobe, R., Parazols, M., Amato, P., Sancelme, M., and Delort, A.-M.: Atmospheric chemistry of carboxylic acids: microbial implication versus photochemistry, Atmospheric Chemistry and Physics, 11, 8721–8733, https://doi.org/10.5194/acp-11-8721-2011, 2011.

Vaïtilingom, M., Deguillaume, L., Vinatier, V., Sancelme, M., Amato, P., Chaumerliac, N., and Delort, A. M.: Potential impact of microbial
540 activity on the oxidant capacity and organic carbon budget in clouds, Proceedings of the National Academy of Sciences USA, 110, https://doi.org/10.1073/pnas.1205743110, 2013.

Voisin, D., Legrand, M., and Chaumerliac, N.: Scavenging of acidic gases (HCOOH, CH$_3$COOH, HNO$_3$, HCl and SO$_2$) and ammonia in mixed liquid-solid water clouds at the Puy de Dome mountain (France), J. Geophys. Res., 105, 6817–6835, 2000.

Vyas, P. and Gulati, A.: Organic acid production in vitro and plant growth promotion in maize under controlled environment by phosphate-
545 solubilizing fluorescent Pseudomonas, BMC Microbiology, 9, 174, https://doi.org/10.1186/1471-2180-9-174, 2009.

Winiwarter, W., Fierlinger, H., Puxbaum, H., Facchini, M. C., Arends, B. G., Fuzzi, S., Schell, D., Kaminski, U., Pahl, S., Schneider, T., Berner, A., Solly, I., and Kruisz, C.: Henry's Law and the Behavior of Weak Acids and Bases in Fog and Clouds, Journal of Atmospheric Chemistry, 19, 173–188, https://doi.org/10.1007/BF00696588, 1994.

Yuan, B., Veres, P. R., Warneke, C., Roberts, J. M., Gilman, J. B., Koss, A., Edwards, P. M., Graus, M., Kuster, W. C., Li, S.-M., Wild,
550 R. J., Brown, S. S., Dubé, W. P., Lerner, B. M., Williams, E. J., Johnson, J. E., Quinn, P. K., Bates, T. S., Lefer, B., Hayes, P. L., Jimenez, J. L., Weber, R. J., Zamora, R., Ervens, B., Millet, D. B., Rappenglück, B., and de Gouw, J. A.: Investigation of secondary formation of formic acid: urban environment vs. oil and gas producing region, Atmospheric Chemistry and Physics, 15, 1975–1993, https://doi.org/10.5194/acp-15-1975-2015, 2015.

Zhai, Y., Li, X., Wang, T., Wang, B., Li, C., and Zeng, G.: A review on airborne microorganisms in particulate matters: Composition,
555 characteristics and influence factors, Environment International, 113, 74–90, https://doi.org/10.1016/j.envint.2018.01.007, 2018.